

Supporting Information

Label-free quantification of intracellular mitochondrial dynamics using dielectrophoresis

Ali Rohani¹, John H. Moore¹, Jennifer A. Kashatus², Hiromi Sesaki³, David F. Kashatus² and Nathan S. Swami¹

¹Electrical & Computer Engineering, School of Engineering & Applied Sciences, University of Virginia

²Department of Microbiology, Immunology and Cancer Biology, University of Virginia School of Medicine

³Department of Cell Biology, Johns Hopkins University School of Medicine, Baltimore, MD

Table of Contents:

(Web Enhanced Object) DEP Movie: Comparison of weak dielectrophoresis for cells with fragmented mitochondria versus strong dielectrophoresis for cells with connected mitochondria

Figure S1: Viability of HEK and MEFs in culture media (DMEM) versus in DEP buffer.

Figure S2: Confirming intact mitochondrial morphology of cells after incubation in buffer for dielectrophoresis (DEP)

Figure S3: Flow cytometry to measure cell size after each genetic modification to alter mitochondrial phenotype

Figure S4: Image analysis for size determination in DEP buffer

Figure S5: Spectral simulations to optimize media conductivity for DEP measurements

Figure S6: Experimental data on effect of media conductivity on DEP spectral distinctions

Figure S7: Comparison of DEP response and mitochondrial features of knockout (KO) versus wild-type (WT) MEF cell lines for the case of Drp and Mfn modifications.

Table S1: Fitted Dielectric parameters for HEK and MEF cells

Figure S8: Calculation of flow rate necessary to enable fluid velocity \sim drag force due to F_{pDEP}

* Corresponding Author. Fax: +1-434-924-8818.

Email: nswami@virginia.edu

S1 – Confirming cell viability and stability of mitochondrial alterations in the DEP buffer:

To ensure viability and intact mitochondrial morphologies within the altered buffer used for the DEP (dielectrophoresis) measurements, we followed the outlined procedures. The HEK cells with Ras (TtH 12V) that express shDrp and the shscramble control were plated on glass coverslips, washed three times with the DEP buffer: 8.8% sucrose, 0.5% BSA plus HEPES, and added DMEM (their normal culture media) to cause media conductivity of 0.15 S/m (1500 $\mu\text{S}/\text{cm}$). Comparison of their viability in this DEP buffer versus the control cells in culture media, as per Fig. S1, indicates that the DEP measurements were performed on representative cells.

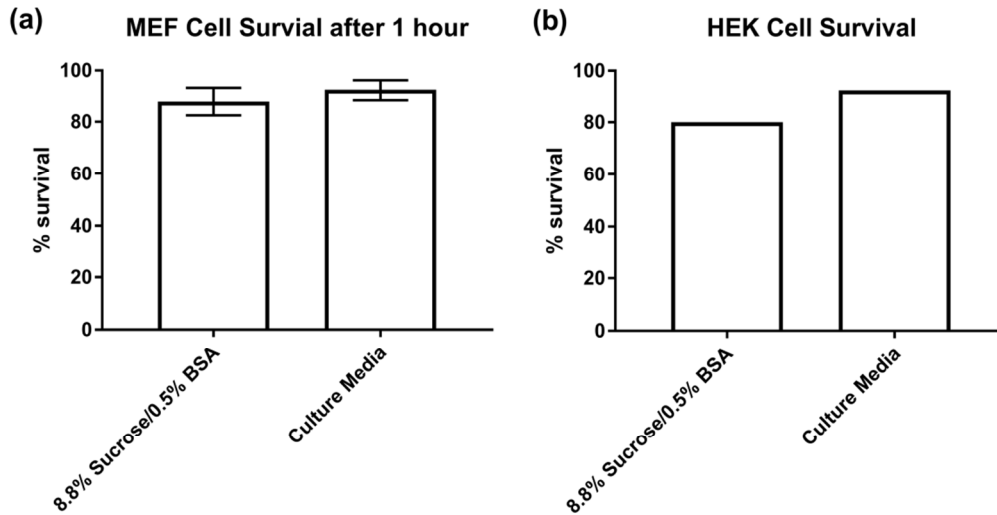


Fig. S1: Viability in culture media (DMEM) versus in DEP buffer for: (a) HEK and (b) MEFs.

For mitochondrial imaging, the respective cells were incubated for 2 hours in the DEP buffer before formaldehyde fixation and mitochondrial staining. The images for both cell types in Fig. S1 show healthy cells with intact mitochondrial morphology that appears consistent with cells in culture media; i.e. HEK Ras cells (TtH 12V) expressing shDrp continue to exhibit elongated mitochondria (Fig. S2a (left)) and those expressing a scramble control continue to exhibit fragmented mitochondria (Fig. S2b (right)). Images of the respective cells in the culture media are shown within Fig. 3.

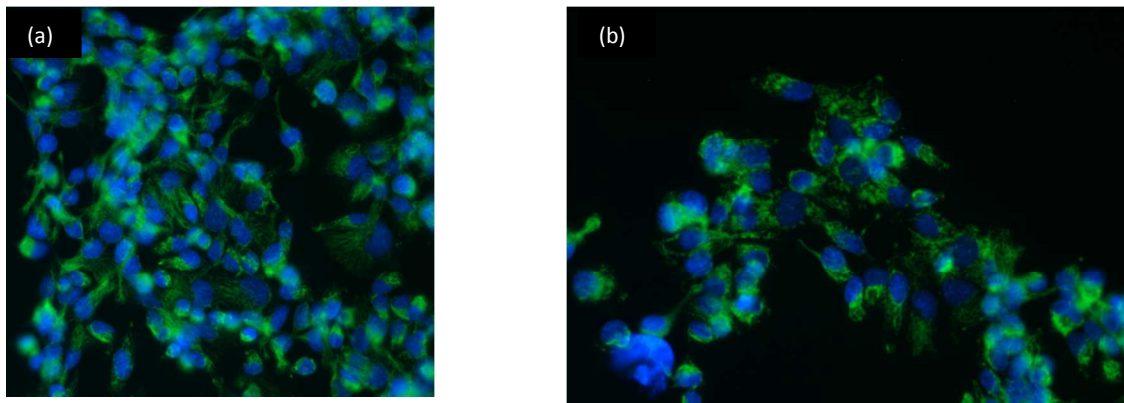


Fig S2: Images of HEK + Ras cells after 2 hours incubation in the DEP buffer, prior to formaldehyde fixation and mitochondrial staining. (a) (Left) shDrp expressing cells continue to exhibit elongated mitochondria and (b) (right) those expressing a Shscramble control continue to exhibit fragmented mitochondria.

S2 – Cell size after genetic modifications to alter mitochondrial phenotype: In order to check on cell size alterations after particular genetic screens to alter the mitochondrial phenotype, we analyzed cell suspensions after each significant alteration using imaging and flow cytometry. The flow cytometry runs from six experiments for each cell type within the histograms of Fig. S3 for forward scatter intensity vs count show close overlaps for HEK+Ras cells expressing shDRP1 versus shScramble control, with a single peak, indicating similar cell size.

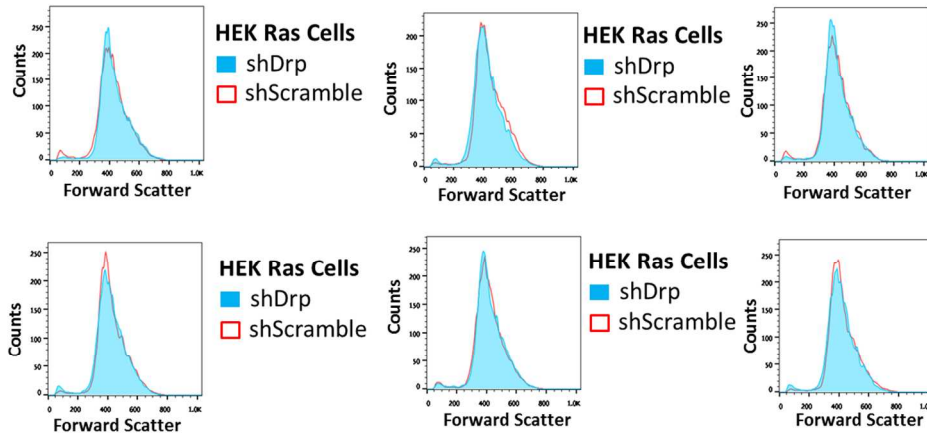


Fig S3. Flow cytometry runs (six experiments with ~10,000 events per experiment for each cell type) shows no significant difference in size of HEK+Ras cells expressing shDRP1 versus shScramble control. The histograms for forward scatter intensity vs count show close overlaps and have a single peak, indicating similar cell size.

As per the images and analysis in Fig. S4, no significant cell size alterations can be discerned for the HEK cells following each significant mitochondrial alteration, as measured based on 30 cells.

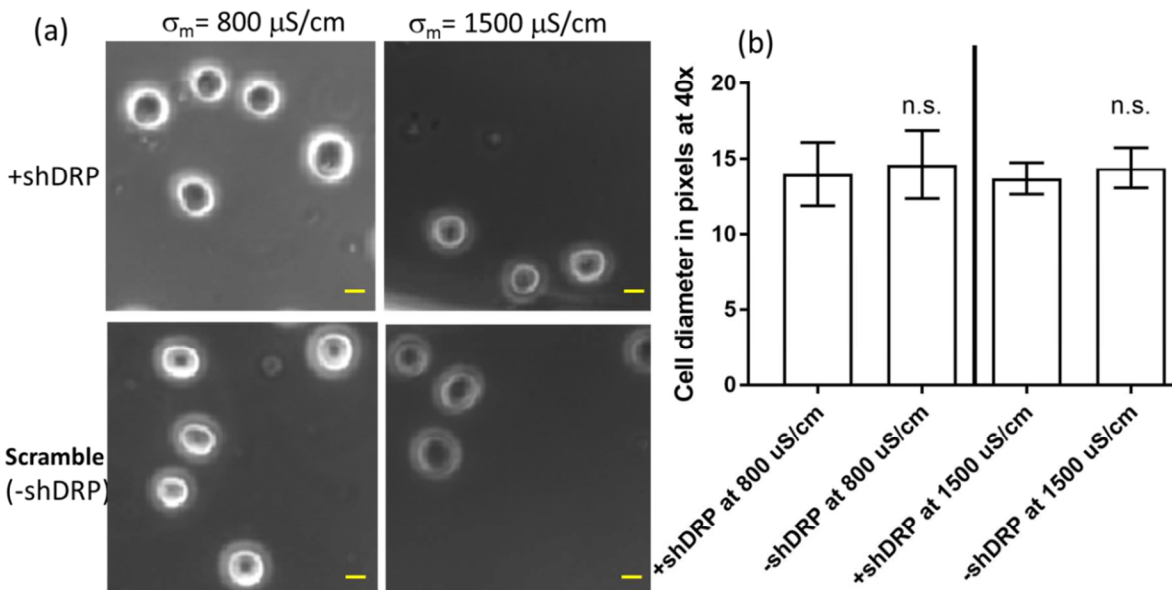


Fig. S4: (a) Suspended cells in DEP buffer: 8.8% sucrose, 0.5% BSA plus HEPES, and added DMEM (normal culture media) to cause media conductivity (σ_m) of 1500 $\mu\text{S}/\text{cm}$ or 800 $\mu\text{S}/\text{cm}$ (under light microscopy at 40x with 10 μm scale bar). (b) Cell diameters were measured using ImageJ software (NIH, Bethesda, MD) in pixels. Three separate images were analyzed to determine if there were differences in cell diameter. A student's t-test was used to determine if there were significant differences ($\alpha = 0.05$) between 30 different cells of +shDRP1 and -shDRP1 at each σ_m .

S3 – Image Analysis to obtain DEP spectra from 3DEP reader: In the 3DEP well system, the internal area of each circular well is divided into 10 concentric circles or bands, from the center to the edge of the well, for analysis of light intensity; with Band 1 being closest to the center and Band 10 being closest to the edge. Under the DEP field at a particular frequency for each well, the light intensity of each circular band in the well from the center to the edge is measured every 1 second, for a total of 30 seconds. Based on this, a 2D map of light intensity for different bands at different times is created by defining X-Axis as the radial distance from the center of the well and the Y-Axis as the time of measurement. This temporal map shows the light intensity at each band along the radius in the well from the center to the edge versus at each time point. Since the accumulation or depletion of particles causes a change in light intensity within different regions of the well, final light intensity at each point is normalized to the background (time = 0), where the field is not yet applied. In addition, since the electric field varies from the center to the edge, a weighting method for normalization of electric field is incorporated to correlate changes in light intensity at each of the different bands. As a result, the DEP force at each band can be compared to measure the relative DEP force at each frequency, at the designated DEP well.

S4 – Optimizing media conductivity for DEP spectral measurements: In this section, we present DEP simulations and spectral data that show the significance of acquiring the data at a critical level of media conductivity (σ_m) to enhance spectral distinctions with varying cytoplasmic conductivity (σ_c) that occur due to mitochondrial morphological alterations.

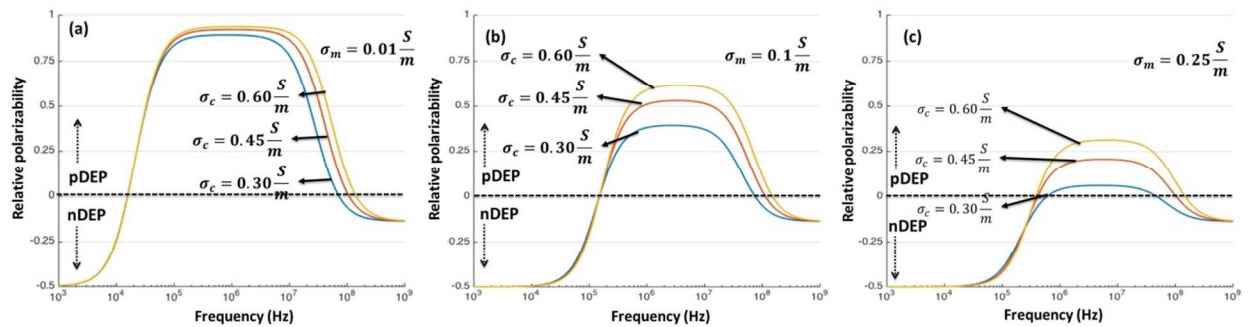


Fig. S5: Spectral simulations of polarizability based on a single-shell dielectric model to investigate the optimal media conductivity (σ_m) needed to enhance the ability for spectral distinctions with cytoplasmic conductivity (σ_c) that occur due to mitochondrial alterations: (a) $\sigma_m=0.01$ S/m; (b) $\sigma_m=0.1$ S/m; (c) $\sigma_m=0.25$ S/m.

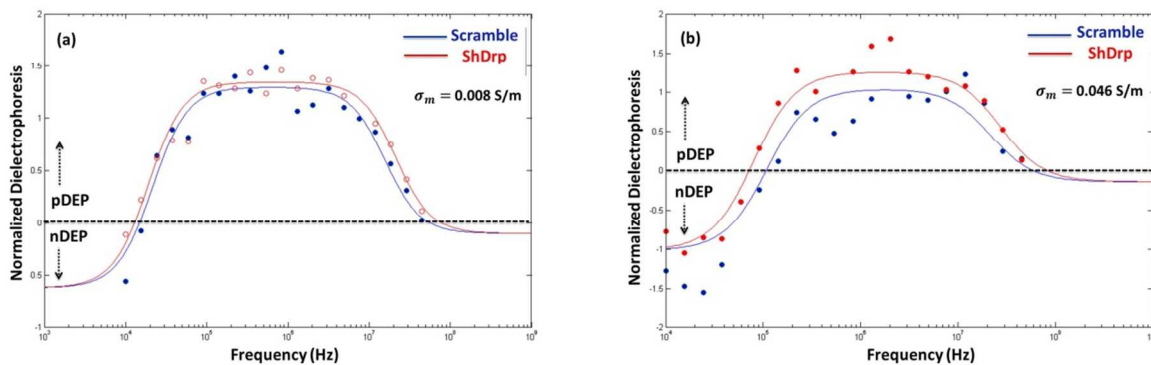


Fig. S6: Effect of media conductivity (σ_m) on measured DEP spectral distinctions due to cytoplasmic conductivity (σ_c) variations, as caused by alterations in mitochondrial morphology. The distinctions are: (a) less clear at σ_m of 0.008 S/m, (b) more clear at σ_m of 0.046 S/m and most clear at σ_m of 0.15 S/m, as per Figure 1a of manuscript.

Figure S5 shows spectral simulations of cell polarizability using a shell dielectric model that is carried out at varying σ_m and σ_c levels. Based on this, it is apparent that variations in spectra with σ_c levels, which are not easily apparent at σ_m of 0.01 S/m (Fig. S5a), become more easily apparent at σ_m of 0.1 S/m (Fig. S5b). At the σ_m level of 0.25 S/m (Fig. S5c), while the distinctions continue to be clear, its proximity to the σ_c value of 0.3 S/m causes the pDEP levels to drop to low levels, which considerably reduces the spatio-temporal variations in light intensity from particle scattering, thereby increasing the error bars on the data acquired on the DEP well measurement system. Hence, the σ_m level of 0.15 S/m was chosen for the measurements reported within the manuscript in Fig. 4a and 4c, since it is close to, but below the range of σ_c levels observed with HEK cells (0.25 – 0.4 S/m) and MEF cells (0.3 – 0.6 S/m) with altered mitochondrial morphologies. In fact, the experimental data from Fig. S6 show improving spectral distinctions for HEK cells from the σ_m level of 0.008 S/m in Fig. S6a versus that measured at 0.046 S/m in Fig. S6b, and the measurement at 0.15 S/m in Fig 4a of the manuscript.

S5 – Mitochondrial network and DEP spectra of knockout versus wild-type MEF cells:

To further ascertain the correlation of the mitochondrial network connectivity to the DEP spectra of MEF cell lines with Drp-KO versus Mfn-KO, we present a comparison of knockout (KO) versus wild-type (WT) for the respective cells (Fig. S7). The mitochondrial connectedness for the WT cells lies between the phenotypes of the respective KO cells, with slightly larger differences in mitochondrial features between Mfn-WT and Mfn-KO versus the respective differences between Drp-KO and Drp-WT. The extreme phenotype observed in the Drp1-KO cell line arises because these cells completely lack fission activity and any fusion that occurs is unopposed. No matter how active the fusion machinery is, the cells will end up with completely connected mitochondria. The reverse is true in the Mfn-KO cells (i.e. unopposed fission). In both sets of wild type cells, the fusion and fission processes are both able to occur, but these processes do not necessarily occur at the same rate. When the fusion machinery and fission machinery are both present, the rates of fusion and fission will depend on the levels of activity of each machinery, which can be influenced by a number of factors. The net “connectedness” of the mitochondria will depend on the “balance” of fusion and fission activity. We can imagine that a cell that has both fusion and fission activity occurring at the same rate will probably have a mitochondrial morphology right between the two extremes (~50% connectedness). The image analysis, as well as the DEP analysis suggests that WT MEFs have slightly more fusion activity than fission activity. Regardless, the end result is a mitochondrial morphology that is not completely connected (like the cells lacking fission activity completely) but it is also not right between the two extremes and is closer to one extreme than the other. This unequal distribution of fission and fusion activity explains why the WT cells are hard to distinguish from the Drp1-KO cells, but they are more easily distinguished from the Mfn-KO cells. Importantly, DEP measurements are able to distinguish extreme mitochondrial phenotypes (Fig. 4b) and the WT controls fall between the two extremes (Fig. S7), for the DEP response and image analysis measurements. This consistency leads us to infer that the pDEP measurements are truly representative of differences in mitochondrial morphology and not another aspect of cell physiology. Follow-up work is underway to measure the DEP response of single cells to improve distinctions, to help parse through any phenotypic heterogeneity *in vivo*.

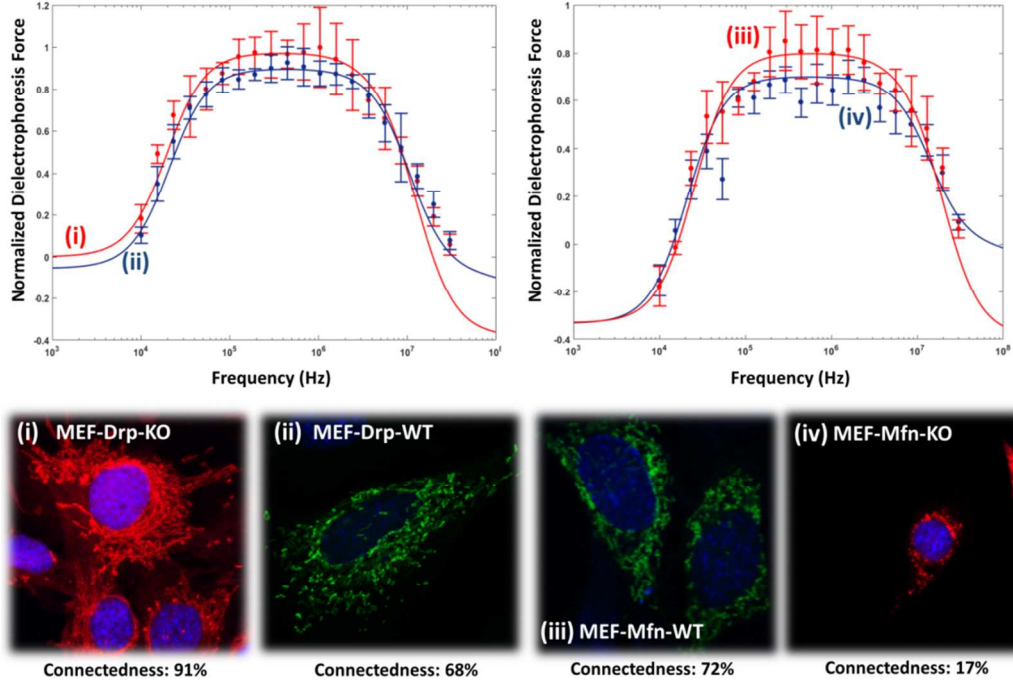


Fig. S7: Comparison of DEP response (top row) and mitochondrial features (bottom row) of MEF-Drp-KO (i), MEF-Drp-WT (ii), MEF-Mfn-WT (iii), and MEF-Mfn-KO (iv) cell lines for the case of Drp and Mfn modifications.

S6 – Geometric and dielectric parameters of each subcellular region: The detailed procedure for fitting the DEP spectra to compute cellular dielectric properties (permittivity: ϵ & conductivity: σ) of each relevant region, based on a three-shell or four-layer dielectric model is presented in the Methods section of the revised manuscript. The respective layers from cell interior to its envelope include: nucleus, nucleus envelope (NucEnvelope), cytoplasm and cell membrane. Herein, we summarize the geometric parameters of each subcellular region that was used to fit the obtained dielectric parameters.

Table S1: Geometric and dielectric parameters (permittivity or ϵ and conductivity or σ of the indicated regions) obtained by fitting DEP spectra to a three-shell or four layer dielectric model, as indicated alongside for a spherical cell. The permittivity values are units of: $\times\epsilon_0$ (F/m), while conductivity values are in S/m units. The media conductivity was fixed at 0.15 S/m.

Parameter (Unit)	Scramble (HEK)	shDRP (HEK)	DRP-Ko (MEF)	Mfn-Ko (MEF)	Geometric parameters of the cell
ϵ_{mem}	14	14	13	13	
σ_{mem} (S/m)	1×10^{-7}	1.1×10^{-7}	6×10^{-5}	8.5×10^{-5}	
$t_{membrane}$ (nm)	11	10	10	9	
$\epsilon_{cytoplasm}$	60	60	60	70	
$\sigma_{cytoplasm}$ (S/m)	0.3	0.52	0.35	0.56	
$R_{cytoplasm}$ (μm)	10	10	10	10	
$\epsilon_{nucEnvelope}$	25	25	25	25	
$\sigma_{nucEnvelope}$ (S/m)	0.9×10^{-3}	3×10^{-3}	1.3×10^{-3}	3×10^{-3}	
$t_{nucEnvelope}$ (nm)	20	20	10	10	
$\epsilon_{nucleus}$	60	60	60	60	
$\sigma_{nucleus}$ (S/m)	1.4	1.4	1.4	1.4	
$R_{nucleus}$ (μm)	5	5	5	5	

S7 – Calculation of necessary flow rate to enable frequency selective isolation of cells: Based on velocity tracking of single-particles under dielectrophoresis towards the constriction tip of the electrode-less DEP device, the electrophysiology for Ras expressing HEK cells caused F_{pDEP} levels that were calculated to be 1 nN due to the mitochondrial modification after shDRP and 0.1 nN due to the mitochondrial modification after shScramble. To calculate the flow rate necessary for selective isolation of cells with F_{pDEP} at the 1 nN level, we need to ensure that the fluid velocity on the cells is significantly higher than the drag force due to F_{pDEP} at the 0.1 nN level. The calculation of this flow rate is performed as follows (see Fig. S8 for device). First, we calculate the velocity due to drag force from F_{pDEP} on each particle type:

$$F_{drag} = 6\pi\eta av$$

$$\frac{Kg \cdot m}{s^2} = 1 \times 1 \times \frac{Kg}{s \cdot m} \times m \times \frac{m}{s}$$

$$10^{-9} = 6\pi(10^{-3})(10^{-5})v$$

$$\frac{10^{-9}}{6\pi(10^{-3})(10^{-5})} = v$$

$$v_{1nN} \approx \frac{0.1}{20} \approx 5 \times 10^{-3} m/s$$

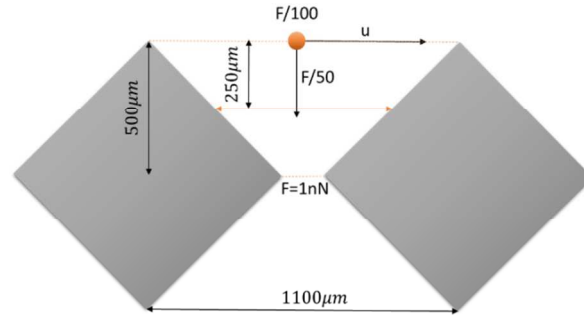


Fig. S8: Force profile across the constriction region of device for calculating flow rate necessary to enable fluid velocity that is comparable to drag force due to pDEP.

Similarly for a particle with 0.1nN force we have:

$$v_{0.1nN} \approx \frac{0.01}{20} \approx 5 \times 10^{-4} m/s$$

While, the DEP force is 1 nN at the constriction tip, we assume a steady drop away from the tip (Fig. S7). For this purpose, it is safe to assume that over a distance of 500 μm from the tip, the DEP force drops 100-fold, so that a linear approximation force of 1/50 can be used along the constricted distance. Hence, the respective velocities at the region just away from the constriction region will be: $v_{1nN} = 100 \mu m/s$; and $v_{0.1nN} = 10 \mu m/s$. Hence, to ensure selective trapping of the particle with the larger pDEP level, we need to adjust the fluid velocity so that this particle will be pulled sufficiently enough toward the constriction (more than half way) during the time required for the particle to cross the insulator wedges at the flow rate of interest, while the particle with the lower pDEP level does not have sufficient time to be effectively pulled toward constriction tip. At 100 $\mu m/s$, particles need 2.5 second to travel the half way toward tips. At its maximum level, it should take ~ 2.5 seconds for the particle to travel 1100 μm along the fluid direction (that is orthogonal to F_{pDEP}).

$$v_{fluid} = \frac{1100}{2.5} \approx 450 \frac{\mu m}{s}$$

Assuming a device depth of 100 μm and spacing between the diamond constriction posts of 500 μm , the necessary flow rate to enable selective trapping can be estimated as 1.35 $\mu L/min$. For cell concentration of 10^5 cells/mL, we can estimate the ability to isolate 135 cells/min (at 100% collection efficiency).